

Mathematical Morphology Aided Optic Disk Segmentation from Retinal Images

Soumyadeep Pal¹ and Saptarshi Chatterjee²

Department of Electrical Engineering
Jadavpur University
Kolkata, India

¹soumyadeepal97@gmail.com, ²saptarshichatterjee2009@gmail.com

Abstract— Computer aided diagnosis has a great impact on detection of pathological conditions and accurate diagnosis of different human eye diseases. The analysis of the anatomy of the optic disk, containing optic cup and optical nerve are very essential for the detection of different diseases like glaucoma, diabetic retinopathy, hypertension etc.. Hence the proper segmentation of the optic disk from the retinal fundus images is an important stage of such diagnosis. In this reported work, a methodological approach has been introduced for the segmentation of optic disk in the retinal fundus images. In the preprocessing stage different color channels of the fundus images have been combined followed by some morphological operations. Canny edge detection technique, assisted with further morphological operations has been used to segment the optic disk. The method has been tested on RIM-ONE database and 94.90% average accuracy and 83.13% Oratio have been achieved.

Keywords— computer aided diagnosis; glaucoma; mathematical morphology; optic disk; segmentation.

I. INTRODUCTION

Glaucoma is a neuro-degenerative eye condition that damages the optic nerve, by building up of pressure inside the human eye. If the damage persists due to the intraocular pressure, glaucoma can lead to the permanent vision loss [1]. However, the diagnosis at an early stage will help to prevent the further damage of the optic nerve head or optic disc (OD) and vision loss. For the diagnosis of glaucoma disease fundus imaging is a gold standard imaging technique for the ophthalmologists. The losses in optic nerve fibers lead to the major structural change in OD. The OD can be divided into two distinct zones, namely, a central bright zone called the cup and a peripheral region called the neuroretinal rim where the nerve fibres bend into the cup region. Cupping or the enlargement of the cup with respect to the OD (thinning of neuroretinal rim) is a distinguishing symptom of glaucoma progression [2]. So, the accurate segmentation of optic disk from retinal fundus images has been consider as an essential step leading to the proper diagnosis of glaucoma using computer aided diagnostic system. In literature different state-of-the-art techniques for the accurate segmentation of OD have been introduced. Joshi *et. al.* proposed an improved OD segmentation method based on region based active contour model, [3]. In [4], a semi-supervised superpixel classification

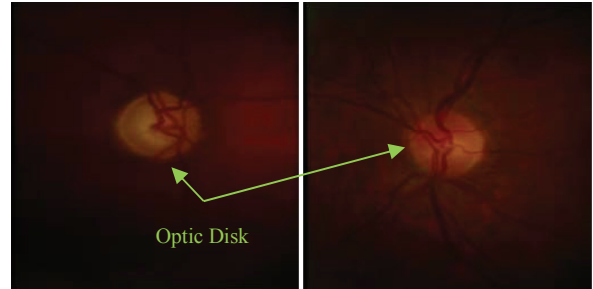


Fig. 1. Sample fundus Images from RIM-ONE database.

technique has been reported for the identification of optic disk and cup regions by Bechar *et. al.* A region-based *MinIMaS* algorithm has been used for the identification and segmentation of the OD region from a retinal fundus image by Roychowdhury *et. al.* [5]. The Markov random field image reconstruction method has been deployed to segment the optic disk by removing the vessels from the optic disk region by Salazar-Gonzalez *et. al.* [6].

In this reported work, a methodological approach has been introduced using mathematical morphology for the segmentation of the optic disk. The proposed work has been verified using the RIM-ONE database containing healthy and glaucomatous fundus images. Sample fundus images have been shown in Fig.1. The main contribution of this methodology is the combination of different morphological techniques to make the fundus image fit for segmentation using simple edge detection techniques. Moreover, different color channels combinations have been introduced to increase the prominence of the optic disk. The importance of the choice of clip limit in the contrast limited adaptive histogram equalization has also been investigated.

The entire paper has been organized as follows. An overview of the database used has been given in section II followed by image preprocessing in section III. In section IV, the optic disk segmentation technique has been discussed and some performance indices for evaluation of segmentation performance have been defined. In section V the results have been discussed with proper justifications and comparison. Finally the paper has been concluded in section VI.

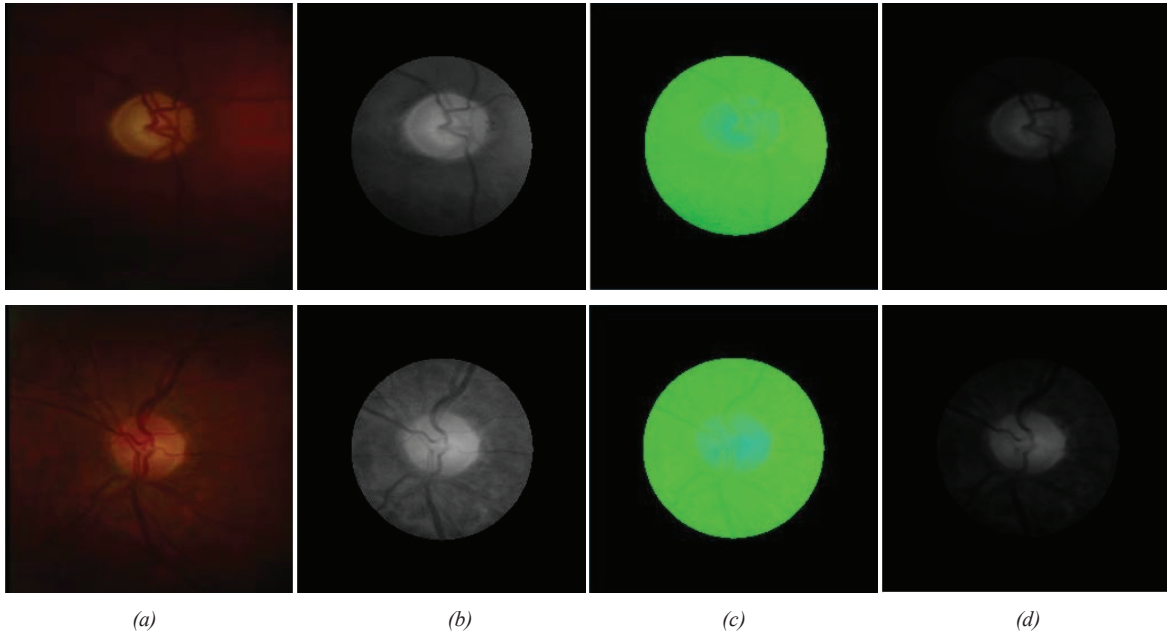


Fig. 2. (a) Original RGB image, (b) red channel of the original image, (c) image in HSV color model, (d) resultant image after pixel by pixel multiplication of red, saturation and value channels.

II. AN OVERVIEW OF THE DATASET

The proposed research work has been carried out using the RIM-ONE public database containing 290 retinal fundus images. The segmentation performance of the proposed methodology has been evaluated based on the ground truth images (optic disk) provided in the database.

III. IMAGE PREPROCESSING

The fundus image has been preprocessed to make it fit for segmentation of optic disk. Combination of different color channels, morphological closing operation followed by histogram equalization technique have been performed in the preprocessing stage.

A. Combining different color channels

The region of interest, which is the neighborhood of the optic disk, has been extracted from the original fundus image. After extracting the red channel from the original RGB images, the median filtering (considering 3×3 neighborhood window) has been performed for the removal of the noise.

The literature suggests that the green channel of the original RGB image provides best prominence of the blood vessels, whereas the red channel provides less contrast between the background and edges of the vessel like structures [7]. As in this work the focus has been given to the optic disk segmentation, the red channel has been considered for fending off the blood vessels. The image has also been converted into the hue-saturation-value (HSV) color model. It has been observed that the saturation and value channel has less prominence of blood vessels inside the optic disk. The value channel of the HSV color model has high optic disk intensity. Considering the advantages of different color channels, pixel by pixel multiplication has been performed between the red, saturation and value

channels of the fundus image. The modified resultant images have been shown in Fig.2. From the resultant images it has been observed that the contrast of optic disk region with respect to the background has been enhanced and simultaneously the vessel like objects have been suppressed.

B. Morphological Closing Operation

The erosion and dilation of a grayscale image X are morphological operations using a structural element B^s , defined as follows [8].

$$\text{Erosion: } X \ominus B^s = \bigcap_{b \in B} X_{-b}$$

$$\text{Dilation: } X \oplus B^s = \bigcup_{b \in B} X_{-b}$$

where, Minkowski subtraction and addition have been denoted by \ominus and \oplus respectively.

The morphological closing of the grayscale image X has been defined as the dilation of the image followed by erosion of the resultant.

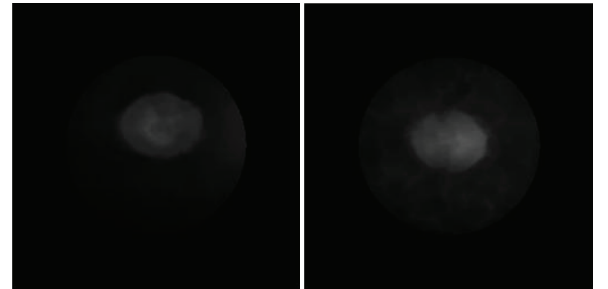


Fig. 3. Preprocessed images after morphological closing and histogram equalization technique.

$$\text{Closing: } X^B = (X \oplus B^s) \ominus B$$

In this proposed work the morphological closing of the image has been performed using a disk shaped structuring element (SE). The intensity of the blood vessels present in the optic disk region have been reduced by the closing operation.

C. Histogram Equalization

After the closing operation, the contrast of the resultant image has been enhanced by using 'Contrast Limited Adaptive Histogram Equalization' (CLAHE) [9] technique. The gradient across the optic disk edges has been increased by introducing the CLAHE algorithm with 8×8 tiles along the entire image. As a consequence, the edges of the optic disk have been further enhanced. The resultant images after the histogram equalization technique have been shown in Fig. 3.

IV. OPTIC DISK SEGMENTATION AND PERFORMANCE EVALUATION

After enhancing the edges of the optic disk region in the preprocessing stage the canny edge detection technique has been employed to obtain the region where the maximum intensity change has been occurred. The double thresholding technique used in canny edge detection method ensured the detection of proper edge location of the optic disk.

The non-uniform intensity distribution along the region of interest has led to the identification of some improper and disjoint edges of the optic disk. Consecutive morphological closing operations with linear structuring element of two pixels distance with horizontal and vertical orientation has been employed for joining the optic disk edges. The final segmented image has been obtained using the flood fill algorithm. The sample segmented optic disk images have been shown in Fig.4. To evaluate the segmentation performance of the proposed methodology the ground truth images provide by the RIM-ONE public database has been used. The segmentation performance evaluating parameters, sensitivity, specificity, accuracy and overlapping ratio or O ratio have been evaluated as follows.

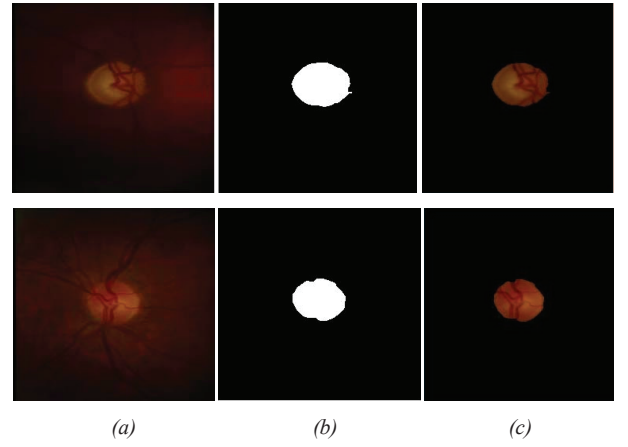


Fig. 4. (a) Original RGB image, (b) final segmented image, (c) image formed after masking the segmented binary image with the original RGB image.

$$\text{Sensitivity} = \frac{\sum \text{correctly classified foreground pixels}}{\sum \text{foreground pixels in ground truth}}$$

$$\text{Specificity} = \frac{\sum \text{correctly classified background pixels}}{\sum \text{background pixels in ground truth}}$$

$$\text{Accuracy} = \frac{\sum \text{correctly classified pixels}}{\text{Total no. of pixels in ground truth}}$$

$$O \text{ ratio} = \frac{G \cap S}{G \cup S}$$

where G is the optic disk boundary from the ground truth while S is the resultant optic disk boundary from segmentation by the proposed methodology.

V. RESULTS AND DISCUSSION

The segmentation performance of the proposed methodology has been evaluated by considering different size of the disk shape structuring elements for morphological operations [10-12]. The size of the structuring elements has been varied from five pixels to ten pixels radius. Values less than five radius have not been considered because of the considerable loss of information and consequently the segmentation performance has also been reduced.

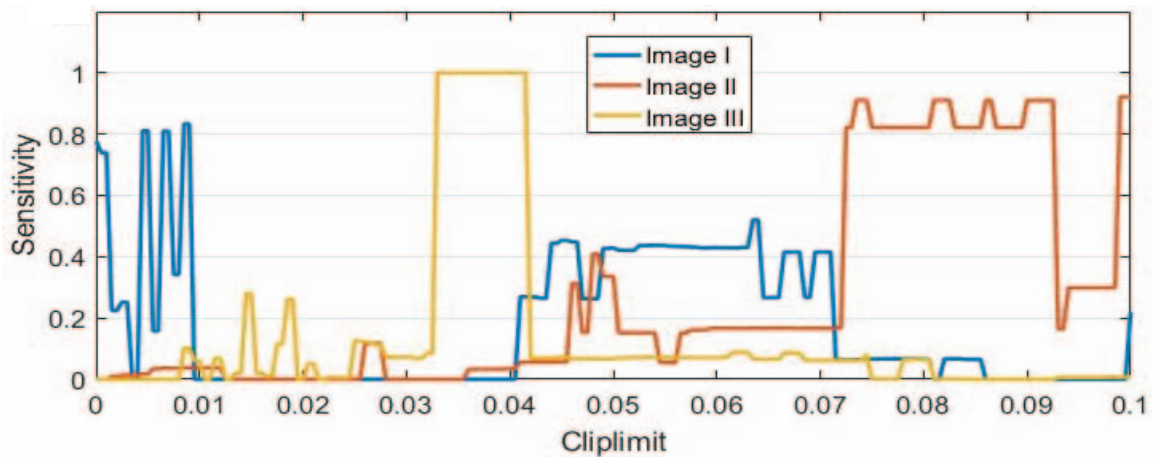


Fig. 5. Variation of sensitivity with cliplimit.

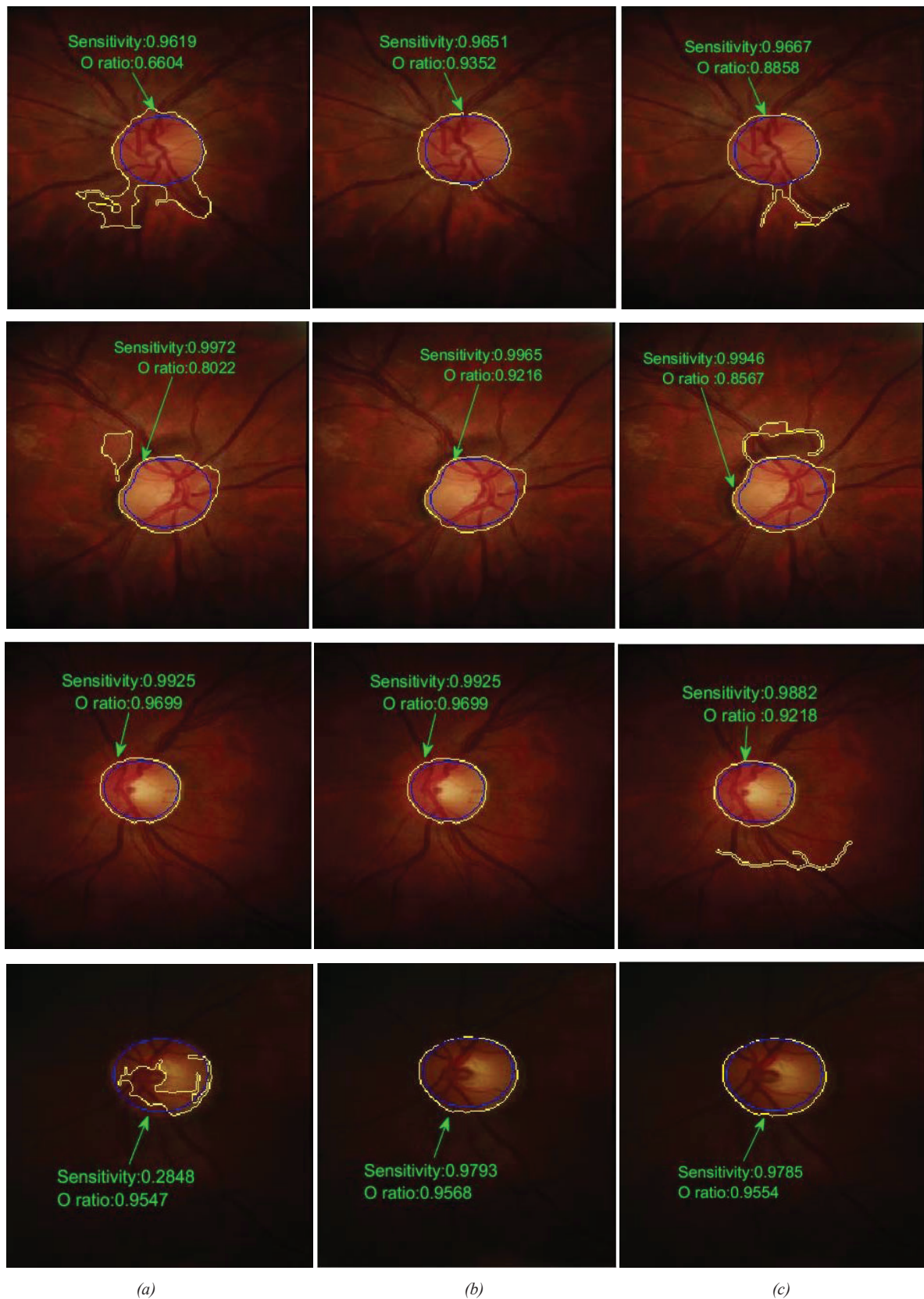


Fig. 6. Comparison of the segmentation performance between the ground truth images and the proposed methodology for the structuring elements of radii (a) 5 (b) 8 and (c) 9. The optic disk boundary from the ground truth has been marked in blue while the optic disk boundary after segmentation from the proposed method has been marked in yellow.

The clip limit of the CLAHE algorithm has also been varied from 0 to 0.1 with an increment of 0.001, until a maximum sensitivity for the segmented image has been obtained. The variation of the sensitivity with respect to the different values of clip limit has been shown in Fig.5 for three sample fundus images. It has been realized that for most of the images the maximum sensitivity has been obtained for clip limit values within 0 to 0.1, and the significant changes in sensitivity have not been noticed beyond the value of 0.1.

The size (radius) of the structuring element has been varied from 5 to 10 pixels distance and at each stage the segmentation performance has been evaluated based on sensitivity, specificity, accuracy and Oratio. In Fig. 6 the optic disk boundary of the ground truth images along with the resultant of the proposed scheme have been shown in blue and yellow color respectively. The variation of the segmentation performances with the size of the structuring element (varied from 5 to 10 pixels radii) has been shown in Fig. 7 and Fig. 8. The variations of the average specificity and accuracy with respect to the size of the structuring elements have been shown in Fig.7. Similarly the effect of size of the structuring element on average sensitivity and Oratio has been represented in Fig. 8. From Fig.7 and Fig. 8 it has been realized that for the size of the structuring element of 8 pixels radius the performance indices achieved the maximum value. The smaller structuring element has not been able to segment the optic disk properly, whereas the larger structuring element has produced over segmentation. Thus, to perform the morphological operations the optimum size of the structuring element has been chosen as eight pixel distance depending on the segmentation performance indices.

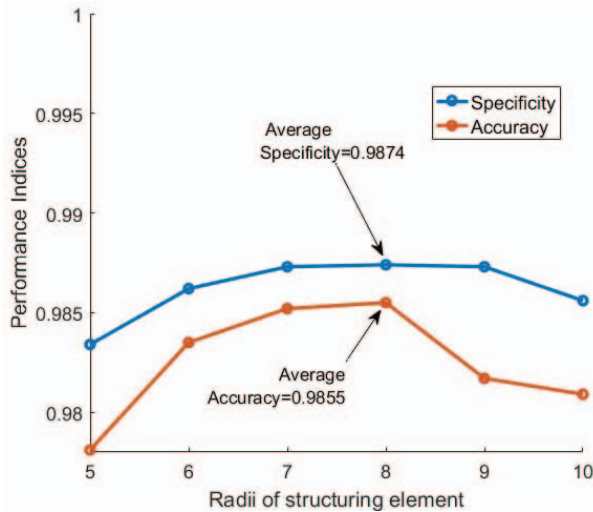


Fig. 7. Variation of specificity and accuracy with radii of structuring element.

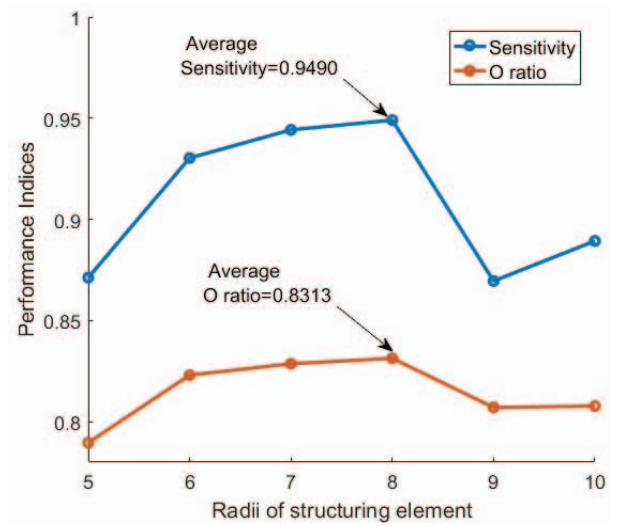


Fig. 8. Variation of sensitivity and Oratio with radii of structuring element.

In Table I the sensitivity, specificity, accuracy and O ratio have been tabulated for twenty sample fundus images among 290 image dataset for the structuring element of 8 pixels radius. The maximum average sensitivity, specificity, accuracy and O ratio have been achieved as 0.949, 0.9874, 0.9855 and 0.8313 respectively. The proposed methodology has been tested on the publicly available RIM-ONE database.

TABLE I. PERFORMANCE INDICES FOR OPTIC DISK SEGMENTATION OF 20 SAMPLE FUNDUS IMAGES WITH STRUCTURING ELEMENT OF 8 PIXELS RADIUS.

#Image_Id	Sensitivity	Specificity	Accuracy	O ratio
1	0.9994	0.9779	0.9790	0.7087
2	0.9876	0.9899	0.9898	0.8229
3	0.9016	0.9793	0.9756	0.6851
4	0.9321	0.9866	0.9836	0.8027
5	0.9746	0.9599	0.9605	0.4969
6	0.9909	0.9813	0.9817	0.7218
7	0.9667	0.9927	0.9912	0.8858
8	0.9946	0.9900	0.9903	0.8567
9	0.9876	0.9945	0.9942	0.9026
10	0.9956	0.9938	0.9939	0.8902
11	0.9907	0.9959	0.9957	0.9156
12	0.5245	0.9920	0.9634	0.8106
13	0.2354	0.9793	0.9445	0.3585
14	0.9957	0.9480	0.9499	0.4404
15	0.2053	0.9873	0.9450	0.4799
16	0.9430	0.9872	0.9854	0.7572
17	0.9863	0.9036	0.9081	0.3665
18	0.9257	0.9818	0.9790	0.7249
19	0.9236	0.9907	0.9871	0.8484
20	0.9898	0.9914	0.9913	0.8474

TABLE II. COMPARISON OF PROPOSED METHOD WITH STATE-OF-THE-ART TECHNIQUES.

Dataset	Different works	Average ORatio	Average Sensitivity
DIARETDB1	Zeng et.al.[13]	0.3843	0.5530
	Welfer et.al.[14]	0.4365	-
	Boykov et.al.[15]	0.5403	0.7635
	Gonzalez et.al.[6]	0.7850	0.8750
DRIVE	Zeng et.al.[13]	0.5591	0.6512
	Welfer et.al.[14]	0.4147	-
	Boykov et.al.[15]	0.5532	0.7398
	Gonzalez et.al.[6]	0.8240	0.9819
RIM ONE	Proposed Methodology	0.8313	0.9490

The proposed methodology has been compared with the other state-of-the-art optic disk segmentation techniques in Table II. Although different datasets have been used by the authors, our proposed methodology has been achieved a comparable segmentation performance with an overlapping ratio of 0.8313 and a sensitivity of 0.9490. In future the proposed scheme will be tested on other fundus image datasets to report a robust optic disk segmentation technique.

VI. CONCLUSION.

In this reported work, a methodological approach has been introduced to segment the optic disk region from the retinal fundus images. In the preprocessing stage, the combination of different color channels followed by morphological operations and histogram equalization technique has been used for the enhancement of the edges of the optic disk region. The canny edge detection has been used to obtain the optic disk boundary that has led to the proper segmentation of the optic disk region. The performance the proposed methodology has been tested for different size of the structuring element with variation of clip limit. The average sensitivity, specificity, accuracy and Oratio have been achieved as 0.9490, 0.9874, 0.9855 and 0.8313 respectively. In future, this method could be used as an important stage for the development of the algorithm for the detection of glaucoma.

REFERENCES

- [1] D. E. Singer, D. Nathan, H. A. Fogel, and A. P. Schachat, "Screening for diabetic retinopathy," *Ann. Internal Med.*, vol. 116, pp. 660–671, 1992.
- [2] R. Bock, J. Meier, L. G. Nyl, and G. Michelson, "Glaucoma risk index: Automated glaucoma detection from color fundus images," *Med. Image Anal.*, vol. 14, no. 3, pp. 471–481, 2010.
- [3] G. D. Joshi, J. Sivaswamy and S. R. Krishnadas, "Optic Disk and Cup Segmentation From Monocular Color Retinal Images for Glaucoma Assessment", *IEEE Trans. On Med. Img.*, vol 30, no. 6, pp. 1192-1204, 2011.
- [4] M. El. A. Bechar, N. Settouti, V. Barra and M. A. Chikh, "Semi-supervised superpixel classification for medical images segmentation: application to detection of glaucoma disease", *J. Multidim. Syst. Sign. Process.*, DOI 10.1007/s11045-017-0483-y, 2017.
- [5] S. Roychowdhury, D. D. Koozekanani and K. K. Parhi, "DREAM: Diabetic Retinopathy Analysis Using Machine Learning", *IEEE J. Biomed. And Health Inform.*, vol. 18, no. 5, pp. 1717-1728, 2014.
- [6] A. Salazar-Gonzalez, D. Kaba, Y. Li, and X. Liu, "Segmentation of the Blood Vessels and Optic Disk in Retinal Images", *IEEE J. Biomed. And Health Inform.*, vol. 18, no. 6, pp. 1874-1886, 2014.
- [7] Nancy M.Salem , Asoke K Nandi, "Novel and adaptive contribution of the red channel in pre-processing of colour fundus images", *Journal of the Franklin Institute*, vol. 334, issues 3-4, pp.243-256, 2007
- [8] P. Soille, "Morphological Image Analysis-Principles and Applications", *Springer, Berlin*, second edition, 2003.
- [9] S. M. Pizer, E. P. Amburn, J. D. Austin, et al., "Adaptive Histogram Equalization and Its Variations", *Computer Vision, Graphics, and Image Processing* 39 (1987) 355-368.
- [10] S. Chatterjee, D. Dey, and S. Munshi, "Mathematical Morphology aided Shape, Texture and Color Feature Extraction from Skin Lesion for Identification of Malignant Melanoma", in *Proc. IEEE CATCON 2015*, Dec., 2015, pp. 200-203.
- [11] S. Chatterjee, D. Dey, and S. Munshi, "Studies on formidable dot and globule detection technique for detection of melanoma from dermoscopic images" in *Proc. Computer, Communication and Electrical Technology, Taylor & Francis Group*, pp. 337-341, 2016.
- [12] S. Chatterjee, d. Dey and S. Munshi, "Development of An Efficient Fractal Based Texture Analysis Technique for Improved Classification of Dermoscopic Images", *Proc. IEEE Uttar Pradesh Section International Conference on Electrical, Computer and Electronics Engineering (UPCON)*, pp. 184-188, 2016.
- [13] Y. Zeng, D. Samaras, W. Chen, and Q. Peng, "Topology cuts: A novel min-cut/max-flow algorithm for topology preserving segmentation in n-d images," *J. Comput. Vis. Image Understand.*, vol. 112, no. 1, pp. 81–90, 2008.
- [14] D. Welfer, J. Scharcanski, C. Kitamura, M. D. Pizzol, L. Ludwig, and D. Marinho, "Segmentation of the optic disk in color eye fundus images using an adaptive morphological approach," *Comput. Biol. Med.*, vol. 40, no. 1, pp. 124–137, 2010.
- [15] Y. Boykov and G. Funka-Lea, "Graph cuts and efficient N-D image segmentation," *Int. J. Comput. Vis.*, vol. 70, no. 2, pp. 109–131, 2006..